Interference of Dual Spillways Operations

Jai Hong Lee, Ph.D., P.E., M.ASCE[1]; Pierre Y. Julien, Ph.D., M.ASCE[2]; and Christopher I. Thornton, Ph.D., P.E., M.ASCE[3]

Abstract: Dual spillway interference refers to the loss of hydraulic performance of spillways when they are placed close together. Spillway interference is examined using both physical experiments and numerical simulations. Stage and discharge measurements from four physical models with dual spillways configurations are compared to the Flow-3D computational results at four dam sites in South Korea. The conjunctive use of two spillways is compared with the singular operation of each spillway. When both spillways are operated at the same time, the total flow rate through the two spillways is reduced by up to 7.6%. Interference coefficients are most significant when the stage H_e exceeds the design stage H_d and when the distance D separating two spillways is short compared to the spillway width W. The parameter DH_d/WH_e correlates very well with the calculated and measured interference coefficients. A flood routing example for the design discharge at Andong dam shows a 42 cm difference in reservoir water level with and without application of the interference coefficient. Consequently, the width of additional spillways (including the interference coefficient) should be increased for dam safety. **DOI: 10.1061/(ASCE)HY.1943-7900.0001593.** *© 2019 American Society of Civil Engineers.*

Author keywords: Ogee spillway; Physical experiment; Numerical simulation; Dual spillway.

Introduction

Spillway performances have been systematically studied since the late 1950s. The US Bureau of Reclamation (USBR) and the USACE Waterways Experiment Station (USACE-WES) published various design charts based on physical model experiments of spillway designs (Li et al. 2011). Numerous dams and spillways were designed with limited hydrological information. As reliable longer-term hydrological records are gathered and improved analysis techniques are available, the inflow design flood (IDF), which is a key factor in designing dams and spillways, is being updated and thus the corresponding increased IDF raises new dam safety challenges.

Recently, the perspective of climate change with increases in localized heavy rain storms has become a major concern to urban populations. Disaster prevention systems designed by previous climate characteristics are being exposed to the danger of floods exceeding the design capacity. Existing dam and spillway structures can become undersized for revised probable maximum floods (PMF). PMF values are consistently being revised and updated taking into account longer record periods, urbanization, and climate change (Koutsunis 2015; Lee and Julien 2016a, b, 2017). To cope with increased floods, such measures as installation of additional spillways, fuse gates, alteration of weir shape, new gates on weirs, enlargement of weirs, and movable weir installations have been implemented in stages around the world. Among them, additional (emergency) spillways are frequently selected as a reasonable model for rehabilitation of dams. However, the design criteria for discharge coefficients and rating curves for dual spillways are not clearly established due to the complexity of the reservoir operation method (ROM) with respect to the design flood (200 year) and the PMF. For the design flood, the constant release-based technical ROM takes into account the flood carrying capacity of the downstream river reach. While during the PMF, all spillways gates are fully opened for the purpose of dam safety.

The updated PMF discharge may require a spillway to have a larger capacity than it was designed for. Constructing an additional spillway next to an existing spillway may reduce the hydraulic performance of both spillways. Spillway interference describes the decrease in flow capacity of two spillways placed close to one another. It is necessary to systematically investigate how both the existing and additional spillways interfere with each other during dual spillway operations. The present study provides the numerical and experimental results of a dual spillway system consisting of an existing spillway (service spillway) and an adjacent additional spillway (emergency spillways). The complex flow characteristics caused by geometry, flow splits, and interference effects of dual spillway configurations make the present analysis a challenging application for hydraulic modeling.

The objectives of this study are outlined as follows: (1) to investigate the performance in terms of discharge capacity of dual spillways through a combination of four physical models and 12 numerical models; (2) to determine stage-discharge rating curves from the physical and numerical models to calculate the interference coefficients from dual spillway operations; and (3) to examine PMF routing at Andong dam and compare the stage differences with and without the interference coefficients during dual spillway operations.

Single and Dual Spillway Performances

Since the first comprehensive laboratory investigation of Bazin (Chow 1959), there has been renewed interest in ogee-crest spillways with hydraulic performance studies covering a diverse range of experimental and computational applications. Also, the majority of the hydraulic information and various design charts derived from

[1]Researcher, Dept. of Civil and Mechanical Engineering, South Carolina State Univ., Orangeburg, SC 29117 (corresponding author). Email: june.lee@colostate.edu

[2]Professor, Dept. of Civil and Environmental Engineering, Colorado State Univ., Fort Collins, CO 80523.

[3]Professor, Dept. of Civil and Environmental Engineering, Colorado State Univ., Fort Collins, CO 80523.

Note. This manuscript was submitted on January 5, 2018; approved on October 30, 2018; published online on March 13, 2019. Discussion period open until August 13, 2019; separate discussions must be submitted for individual papers. This paper is part of the ***Journal of Hydraulic Engineering***, © ASCE, ISSN 0733-9429.

extensive data taken from hydraulic model tests have been published and updated by the USBR and the USACE-WES. In a diagnostic study on the hydraulic behavior of spillway flow, Cassidy (1965) calculated the crest pressures and free surface showing good agreement with experimental data using potential flow theory with mapping into complex plane. The findings led by Cassidy indicated that viscosity has no effect on the location of the free surface and the boundary configuration affects the minimum pressure point for a given head. Olsen and Kjellesvig (1998) completed additional improvements on the two-dimensional (2D) and three-dimensional (3D) modeling for spillway flow behavior by numerically solving the Reynolds-averaged Navier-Stokes (RANS) equation and using k − epsilon turbulence closure, and compared discharge coefficient and pressure distribution of spillway surface with empirical formula and physical model measurements. From the comparative analyses of flow over a single ogee-crest spillway using a combination of empirical theory, numerical simulation, and physical model test, Savage and Johnson (2001) estimated the discharge and pressure, and found a general agreement between the computed and measured data. Chanel and Doering (2008) investigated the discharge characteristics over an ogee-crest spillway using computational fluid dynamics (CFD) codes and compared the results with physical model measurements with respect to profiles. More recently, Ho et al. (2006) provided an overview of how the numerical modeling approach was applied to a number of spillway upgrade projects in Australia. With a pseudovalidation process, they highlighted the reliability of the numerical model studies with various analysis capabilities for better understanding of the spillway flow behavior. Also, Zeng et al. (2017) presented a computational approach by the parallel, pressure-based, nonhydrostatic commercial code ANSYS Fluent, to obtain numerically generated data of spillway flow ratings for complementing field measurements, and demonstrated close agreement between computed and measured data.

Most previous studies on ogee spillways have focused on the hydraulic characteristics of singular spillway discharge performance. Also, these studies have primarily focused on service spillways. The literature on dual spillways is nonexistent and the concept of dual spillway interaction is novel. In this analysis, we have focused on the outflow condition of a service spillway and an additional spillway under the extreme flood events. The additional spillway, such as emergency spillways, functions only when extreme flood events occur at the proposed dam basin area. To cope with increased floods, namely the IDF based on the PMF, full opening of all spillways' gates is applied as a reservoir operation method for the purpose of dam safety. In addition, the sill elevation of the emergency spillway is practically designed the same as that of the existing spillway for the purpose of the consistent operation condition. In this study, dual spillway operation was applied to the case of uncontrolled free flow and spillways with the same sill invert elevations between existing and additional spillways.

Fig. 1 defines the separation distance D between two spillways of total combined width, $W = L_E + L_A$. The interference effect due to the simultaneous operation of two spillways (called dual spillway operation) is expected to become significant as the distance D becomes small. The outflow discharge Q_E is through the existing spillway, and Q_A is the outflow discharge through an additional spillway. Also, Q_{E+A} denotes the total simultaneous outflow discharge through both the existing and additional spillways, while $Q_E + Q_A$ is the summation of outflow discharges through the existing spillway and additional spillway, respectively. As shown in Fig. 2, plotted from physical model data, Q_{E+A} is less than $Q_E + Q_A$ due to the interference effects of dual spillway operations. In other words, hydraulic experiments simultaneously operating both the existing and additional spillways, show that the

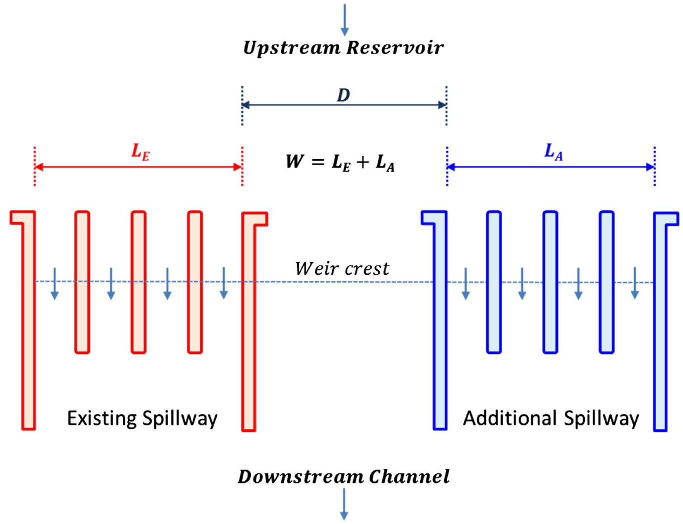

Fig. 1. Definition sketch for dual spillways.

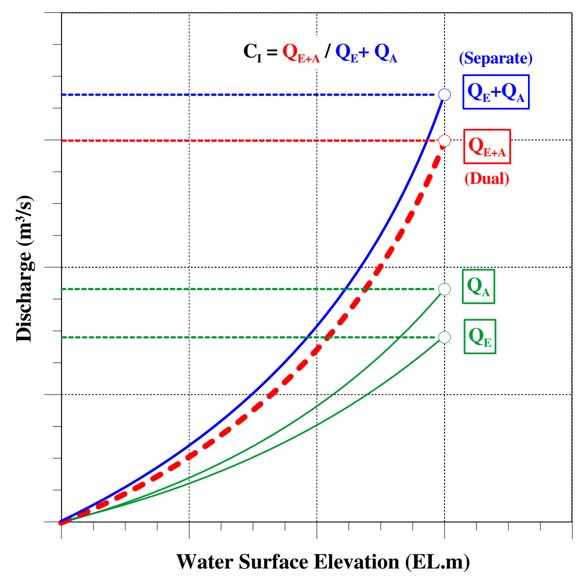

Fig. 2. Stage-discharge rating curves for dual spillway operations.

efficiency of the outflow discharge through the two spillways is reduced. Detailed results and reduced effectiveness of discharge capacity through the existing and additional spillways is shown in the following sections. To quantify the interference effects of dual spillways, interference coefficient $C_I = Q_{E+A}/(Q_E + Q_A)$ is defined for dual spillway configurations with the same crest elevation.

Physical Modeling

The empirical estimates and numerical simulations were performed for the configurations of dual spillways at four major dams in South Korea: Juam dam, Andong dam, Imha dam, and Soyanggang dam. As shown in Fig. 3, four physical models were constructed for the first three dams. In the case of Soyanggang dam, an existing reference to the physical modeling report of MOCT (2003) was used. Physical experiments were performed at the Rural Research

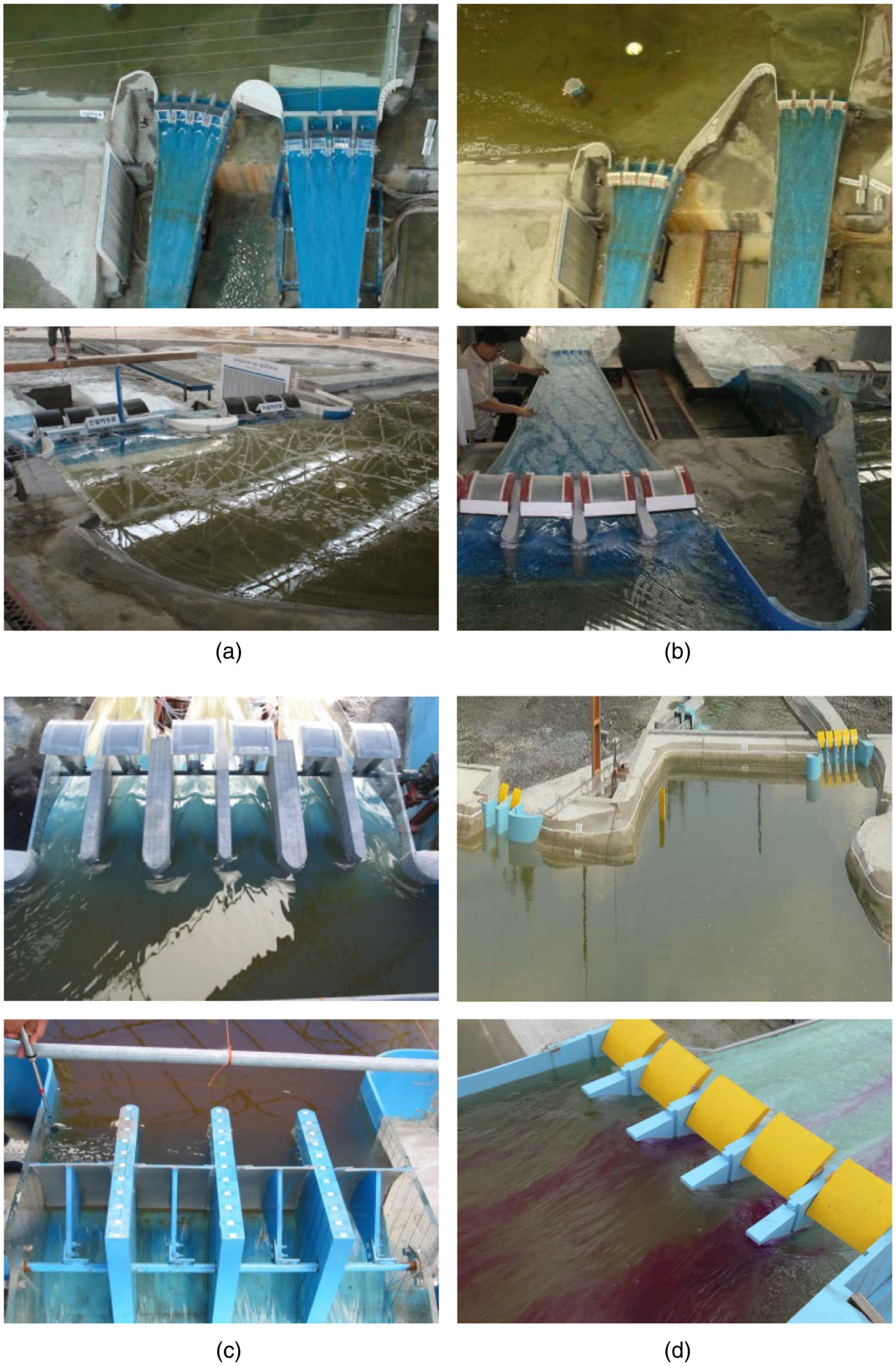

Fig. 3. Physical modeling of dual spillways: (a) Andong-1; (b) Andong-2; (c) Imha-1; and (d) Juam-1.

Table 1. Similitude for physical experiments and prototype-model ratios

Variables	Symbols	Ratio	Andong	Juam	Imha	Soyang
Length	L = length	S_L	1:70	1:70	1:70	1:50
Discharge	Q = velocity × area	$S_L^{5/2}$	1:40,996	1:40,996	1:40,996	1:17,678
Model scale	A = area	S_L^2	1:4,900	1:4,900	1:4,900	1:2,500
Time	U = length/time	$S_L^{1/2}$	1:8.367	1:8.367	1:8.367	1:7.071
Velocity	t = length/velocity	$S_L^{1/2}$	1:8.367	1:8.367	1:8.367	1:7.071
Pressure head	P_h = length	S_L	1:70	1:70	1:70	1:50

Table 2. Model scales for physical and numerical modeling

Variables	Unit	Andong	Juam	Imha	Soyang
Boundary area (physical model)	m^2	1,500,000 (305)	1,000,000 (204)	1,200,000 (245)	500,000 (200)
Maximum discharge (physical model)	m^3/s	11,193 (0.273)	9,983 (0.244)	13,500 (0.329)	13,500 (0.764)
Gate dimension (physical model)	$m \times m$	16.8×12.5 (0.24×0.18)	13.7×14.5 (0.20×0.21)	11.8×14.8 (0.17×0.21)	14.0×13.0 (0.28×0.26)
Weir net width (physical model)	m	67.2 (0.96)	27.3 (0.39)	70.8 (1.01)	56.0 (1.12)
Design head (physical model)	m	10.7 (0.15)	12.0 (0.17)	13.3 (0.19)	12.5 (0.25)
Weir crest elevation (physical model)	EL.m	151.0 (151.0)	98.5 (98.5)	151.4 (151.4)	185.5 (185.5)
Numerical model size	m	x:2,665 y:1,810 z:80	x:1,120 y:1,200 z:95	x:1,300 y:1,400 z:140	x:3,300 y:1,850 z:135
Numerical model meshes	ea	x:250 y:230 z:35	x:160 y:185 z:40	x:165 y:180 z:55	x:210 y:88 z:27

Note: EL.m = elevation of 00.0 m.

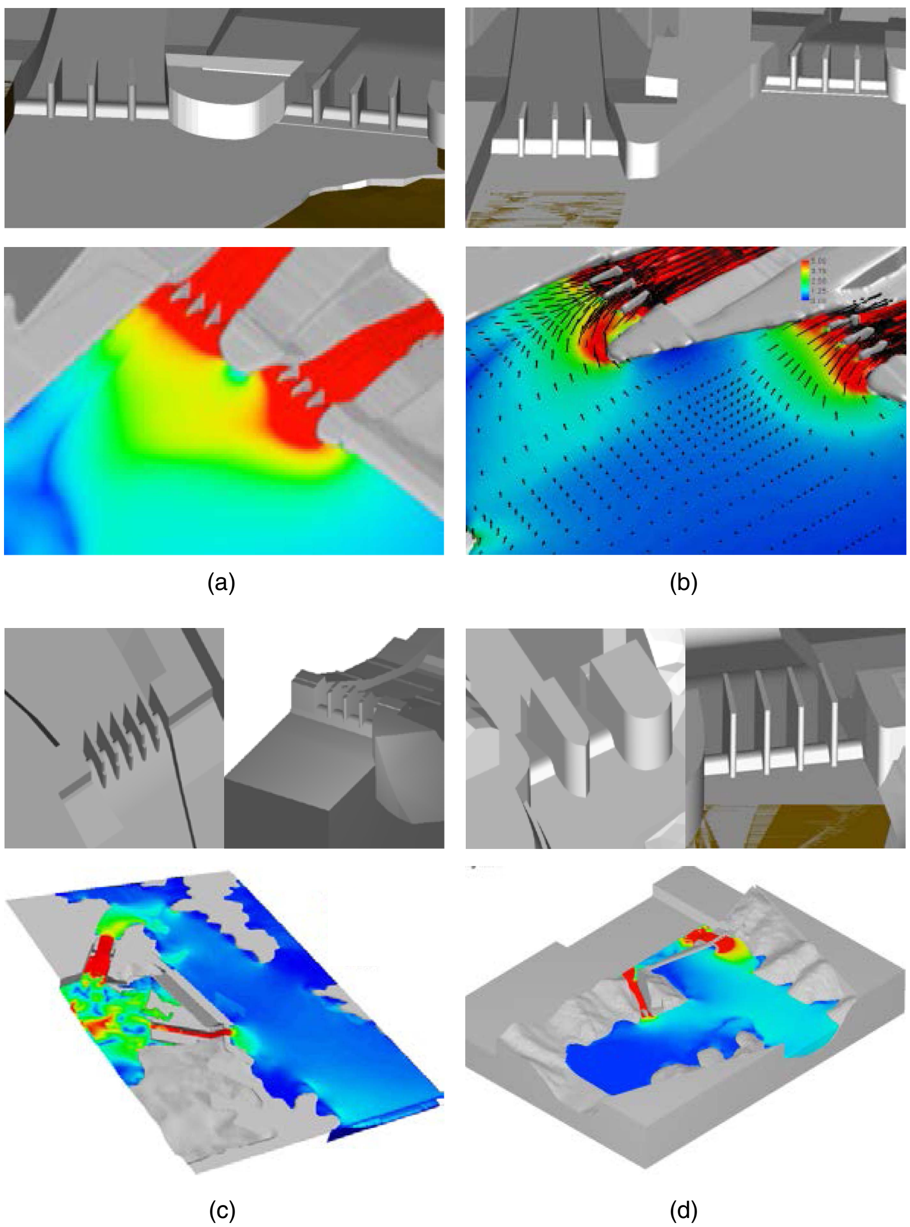

Fig. 4. Numerical modeling of dual spillways: (a) Andong-1; (b) Andong-2; (c) Imha-1; (d) Juam-1; (e) Andong-3; (f) Imha-2; (g) Imha-3; and (h) Juam-3.

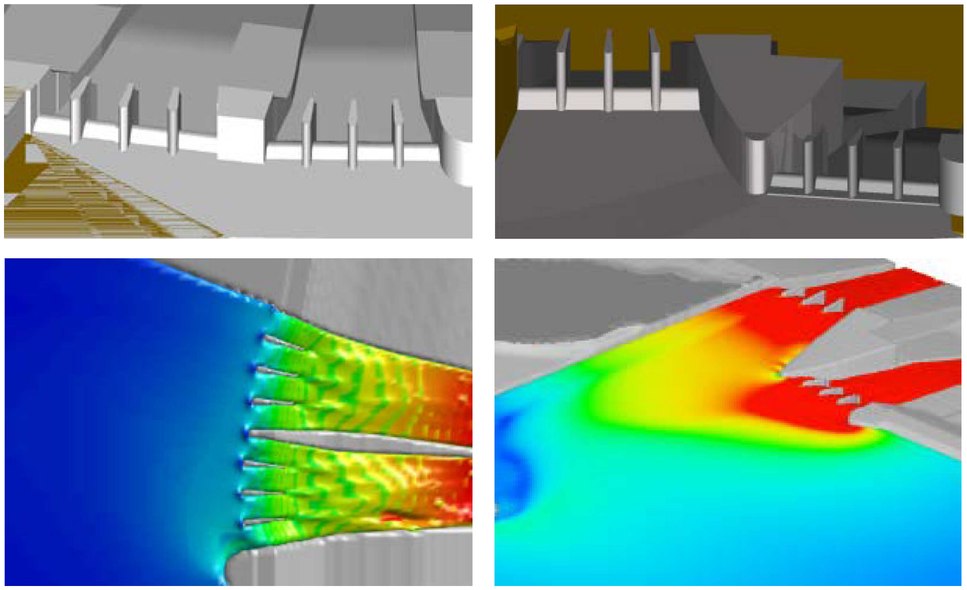

(e) (f)

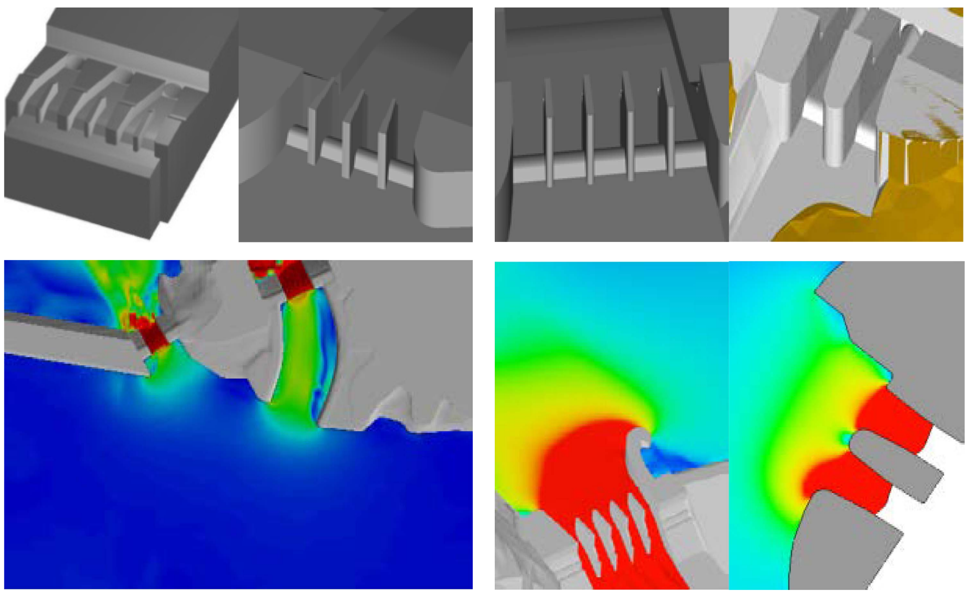

(g) (h)

Fig. 4. (*Continued.*)

Institute laboratory located in Ansan-si, Gyeonggi-do, for the four spillway configurations at the aforementioned dams. Physical models of the ogee crests of existing and additional spillways with a design head H_d were constructed and fabricated using plexiglas walls and steel bottoms considering distinctive shape of the proposed weir crest as shown in Tables 1 and 2. Generally, physical model similarity is achieved and experiments are performed using Froude number similarity in the hydraulic model study on the open channel flow and hydraulic structures. Inappropriate scale model causes a failure to simulate the forces attendant to fluid properties (e.g., viscosity, surface tension) resulting in different flow behavior than that of a prototype. A suitable scale factor must be chosen for the hydraulic model. The USBR (1980) recommended length scale ratios of $L_r = 30–100$ for models of spillways on large dams. In this study, the physical models were constructed on scale ratio of 1:70 considering laboratory space and the aforementioned guidelines suggested by USBR (1980). In addition, an entrance channel, a tangent sectional control structures, and discharge channels were modeled. In this test, plexiglas was used taking into account the fact that it could replicate the smooth curves, and be clearly observed by test facilities. To keep a uniform approach flow, wave suppressors and baffles were installed in the flat bottoms of the water supply flumes. Besides control valves to set the flow in the models, in order to control the flow rate to the model and accurately measure the flow rate, a full width sharp-crested weir was installed at the inlet of the model with a piezometer on the side of the inlet flume. Measuring devices for velocities and water surface elevations in the upstream reservoir were point gage, a 2D electromagnetic meter and micropropeller current meter. Piezometers with glass tubes, which are vented to the atmosphere, were used for measuring pressures on the spillway. The tests were performed at various flow head ratios, H_e/H_d, representing the ratio of the actual head above the crest including the velocity head for the design discharge. Each hydraulic experiment was conducted at six different upstream flow head conditions ranging from $H_e/H_d = 0.2$ to 1.33.

Numerical Modeling

The numerical simulation through a commercially available CFD program, Flow-3D, was performed for the previously proposed dams equipped with an existing service spillway and an additional emergency spillway with 12 various scenarios with respect to topographical layouts of each spillway as shown in Fig. 4. For hydraulics applications, the CFD modeling with prototype dimensions is implemented by solving the governing equations describing the incompressible flow behavior based on the conservation of mass and momentum, e.g., continuity equations and momentum equations known as Reynolds-averaged Navier-Stokes equations. For tracking free surface of air and water interface with respect to time and space, the volume of fluid (VOF) technique is used, making up of each cell in the mesh to the conditions of full, empty, and partially filled with water. Similar to the VOF method, the fractional area volume obstacle representation (FAVOR) function is employed for modeling complex geometric regions, classifying the porosity condition of each cell into three categories, namely without obstacles, with obstacles, and partially filled with the obstacles. With VOF and FAVOR variables for incompressible flow, the continuity equations and the Reynolds-averaged Navier-Stokes equations are expressed as illustrated in Eq. (1)

$$\frac{\partial}{\partial x_i}(u_i A_i) = 0, \qquad \frac{\partial u_i}{\partial t} + \frac{1}{V_f}\left(u_j A_j \frac{\partial u_i}{\partial x_j}\right) = \frac{1}{\rho}\frac{\partial P}{\partial x_i} + g_i + f_i \tag{1}$$

where u_i = velocities in x_i coordinates (x-, y-, and z-directions); A_i represents fractional areas in each subscript coordinate; V_f = fluid volume fraction; and P, ρ, g_i, and f_i = pressure, density, gravitational force, and Reynolds stresses for turbulence closure, respectively.

In each cell, the face areas (A_i) and volume fractions (V_f) are equal to 1 when the cells are completely full of fluid so that the equations are reduced to the basic incompressible RANS equations. The computational mesh is defined as a hexahedral grid of variable-sized cells in Cartesian coordinates. Through a staggered grid technique, average values for the velocity and pressure for each cell are calculated at discrete times. All dependent variables are located at the center of each cell, while velocities and fractional areas are placed at the center of each cell face normal to the corresponding direction. The renormalized group (RNG) energy dissipation equation was selected as turbulence closure model as a follow-up to the methodological approach by Yakhot and Orszag (1986) and Yakhot and Smith (1992).

When conducting the simulation of spillway flow, it is most important that the model of reservoir and spillway structure should be replicated accurately. For the three-dimensional numerical simulations, both hydraulic structures and geometry must be represented by a three-dimensional grid in accordance with the proposed spillways and topographical shape of upstream reservoir based on the area-capacity relationship. In this study, the 3D bathymetry has been taken into account for 3D CFD simulation. The modeling process for the spillway structures consists of an analysis of design drawings, polylining of spillway structures, three-dimensional solidification of polylines, and positioning. Three-dimensional surfaces in a stereolithographic (STL) computer aided design (CAD) format were generated based on the x-, y-, and z-directions data, and correspondingly three-dimensional solid models were constructed for each region. The spillway downstream was simplified because the flow of the downstream end does not have an effect on the flow upstream over the control structure. The radial gates installed on the ogee-crest weir of the spillways were not included because they will be fully opened by the time the reservoir outflow reaches its peak discharge. However, the bridge piers and abutments were included in the model, taking into account their influence on the spillway overflow characteristics. Because the approach channel, control structure, and discharge channel are generally constructed of concrete, the roughness height is selected as 0.5 mm following the comparative results reported by Kim and Park (2005). A fine grid size of 1–2 m was employed in the region of high velocity flow over the ogee-crest spillway showing acceleration and subcritical to supercritical transition flow, as well as in the area of a partially submerged approach channel and guide walls of the spillways because they have a great effect on inflow characteristics in front of the spillway. Also, a coarser than 3 m grid was used in the simple geometry and flow region. The calculation domain and mesh configuration are described in Table 2 and Fig. 5. The three-dimensional computational domains beyond which the boundary effect related to the spillway structural and geomorphic configuration are negligible, were determined based on the 2D simulation results for the upstream and reservoir on the PMF flow condition. The proposed model was structured 2.5–4.0 m higher than the target maximum water level (MWL) for PMF in order to allow the water surface to rise but prevent the water from spilling out of the calculation domain.

To model the flow, boundary conditions are established for each side of the computational space. Hydrostatic pressure was adopted for the upstream boundary condition, the atmospheric pressure condition for the top, the outflow for the downstream boundary condition, the wall boundaries with no slip for the sidewall, the bottom wall, the gate pier, and the ogee crest. The CFD modeling uses unsteady state simulation to reach a steady state. If the initial

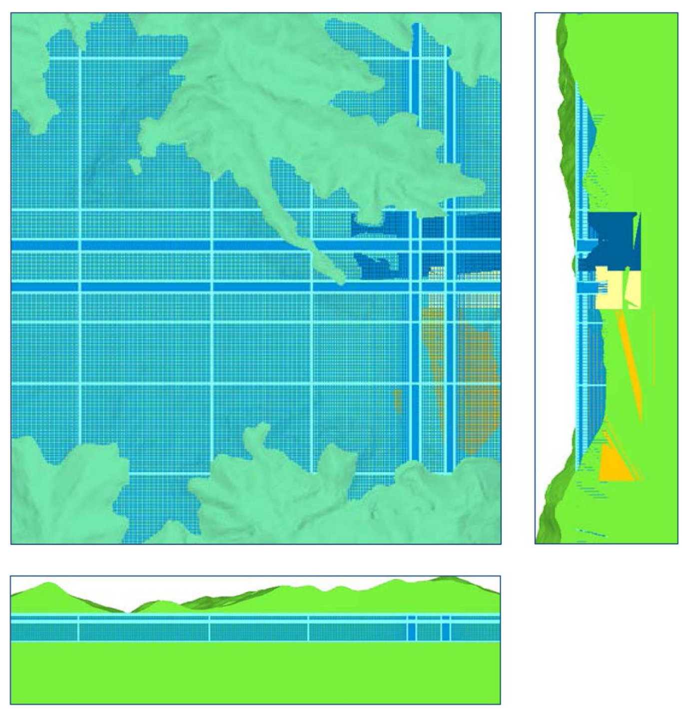

Fig. 5. Meshes and calculation domain for numerical modeling of Andong dam.

condition is largely different with the final steady state solution, simulation can be time consuming. Therefore, the initial conditions are very important to reduce the simulation time. In this study, a commonly used initial boundary condition was set up such that an initial block of water corresponding to the upstream head is located in the upstream side of the spillway with a vertical wall of water standing at the crest. The transient flow analysis was performed with this wall of water rushing down the crest toward downstream.

Physical and Numerical Models Comparison

For the same spillway condition, we can compare the stage-discharge relationship obtained from the numerical model and from the physical experiments. For a comparison in a simplest form, the resulting values were transformed into dimensionless parameters. The parameters H_d and Q_d represent the design head (m) and the design flow rate (cms) through the weir crest, respectively. These parameters from the physical models are used as the basis. Fig. 6 displays the stage-discharge relationship. The flow rate Q is divided by Q_d and shown on the ordinate, while H_e, which is the effective head including the approach velocity head, is divided by the design head H_d and shown on the abscissa. As shown in Fig. 6, the results of analysis for the existing and additional spillways show good agreement for the physical model experiment and the numerical simulation. Based on the physical experiment and its flow rate as the observed standard, Fig. 7 comparatively depicts the four calculated and measured results at the existing spillway and the additional spillway. Fig. 7 also shows the relative root-mean square error (RRMSE) and coefficient of determination (R^2) between physical and numerical modeling

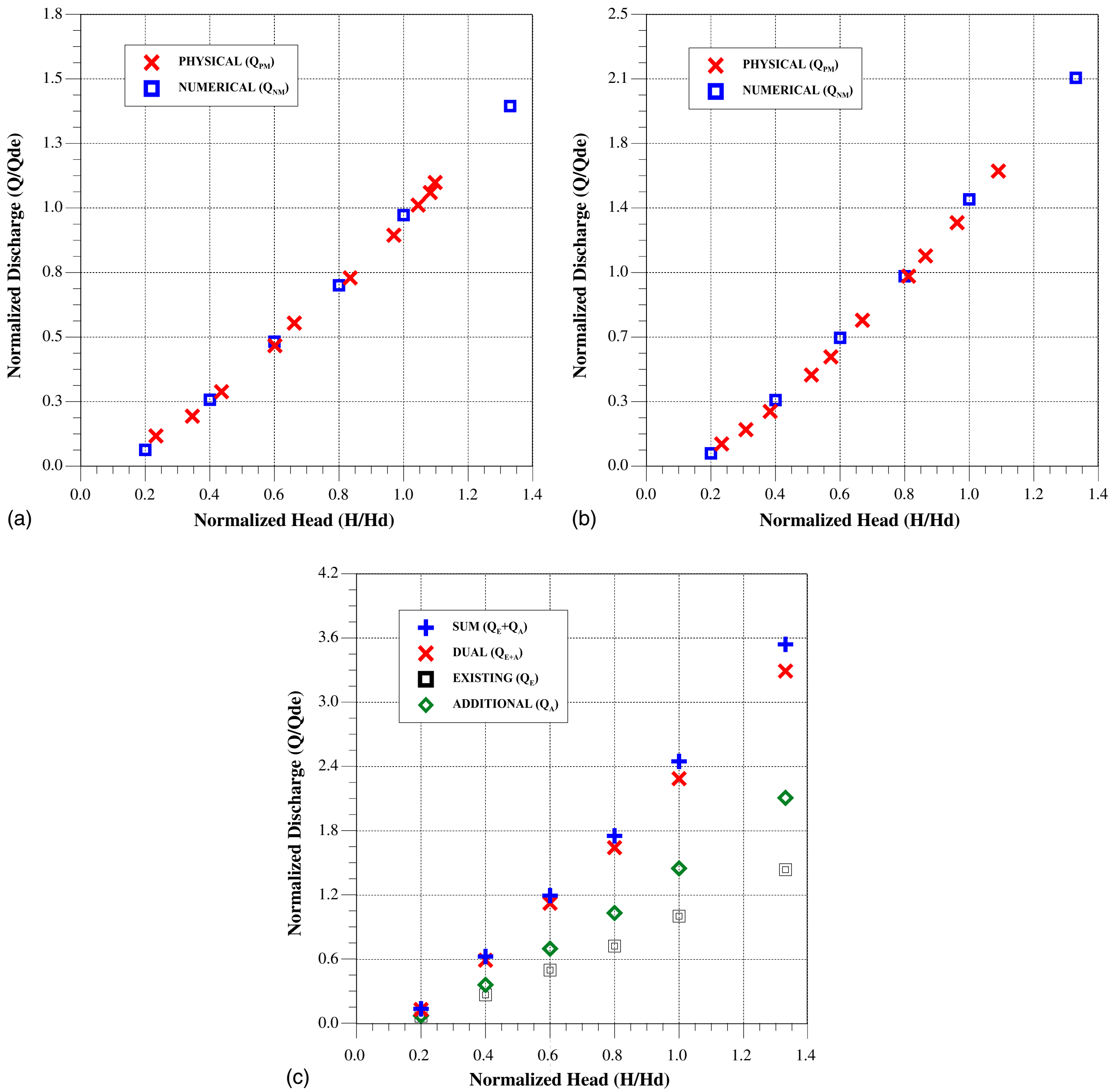

Fig. 6. Stage-discharge rating curve for existing and additional spillways (Andong-1): (a) existing spillway; (b) additional spillway; and (c) dual spillway simulations.

results. The results from the physical experiment and the numerical simulation fall on or near the line of perfect agreement with successful R^2 and RRMSE values for all four simulations. It can be observed that the computed results gave a slightly higher discharge, but the general trend and magnitudes are in good agreement with the physical model experiments. For model calibration and validation studies, the physical model experiment is still essential despite the fact that it may be more expensive and time consuming than the numerical simulation. The numerical model studies provide specific and detailed information of the flow characteristics of hydraulic structures. For the cases considered in this paper, the numerical modeling approach provided a close agreement with measured stage-discharge relationship by physical model tests. Correspondingly, based on the comparative analyses between the physical and numerical model studies, the stage-discharge rating curves for the proposed cases were calculated using numerical simulation results validated by physical model studies to investigate the interference induced by the dual spillway operation under PMF conditions.

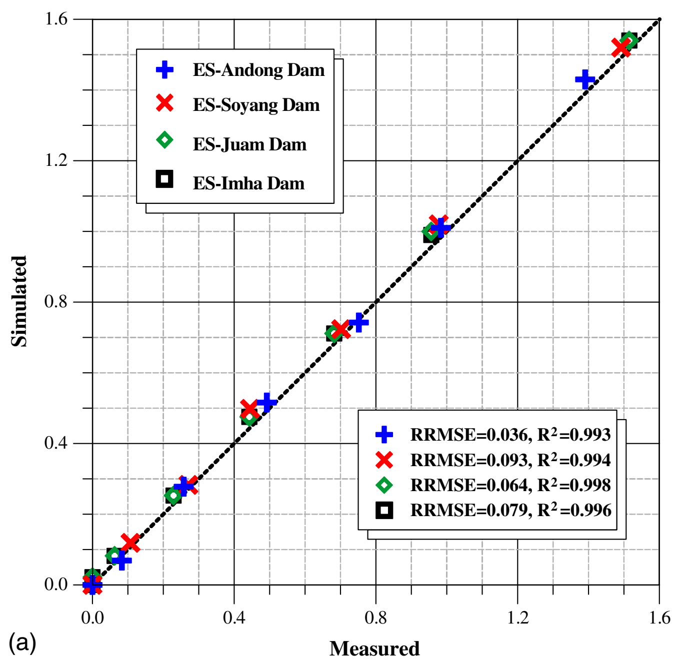

Fig. 7. Discharge comparison of physical experiments and numerical simulations. The upper panel is the comparative result for the existing spillway (ES) and the lower panel is for the additional spillway (AS) at four dams.

Data Analysis

To identify the interference effects on the discharge capacity of dual spillways, a combined factor for the distance and width of two spillways was selected taking into account the topographical layout of spillways' configuration. This is the distance-width ratio (D/W) between the existing and additional spillways. With respect to the distance-width ratio (D/W) between the two spillways, the total scenarios for comparison of physical and numerical results are composed of 12 cases as shown in Table 3.

The primary focus of the analysis was to demonstrate a complementary analysis through physical experiments and numerical simulations for flows over an uncontrolled ogee crest. Existing USBR data have also been included in the comparison to existing references. According to weir sizes of existing and additional spillways, the outflow discharges with respect to water surface elevation of the reservoir were calculated as shown in Table 4. The comparative analysis for existing and additional spillways shows good agreements between the hydraulic experiments and the numerical simulations at design head. Also, Fig. 6 shows that when both the existing and additional spillways are operated simultaneously, the total flow rate through the two spillways is reduced by up to 7.6% at a given water depth. Consequently, the flow rate over the two spillways has a tendency to decrease under simultaneous operations of the two structures.

As a quantification of interference effects of dual spillways, an interference coefficient was used to take into account the topographical layout of dual spillways configurations. Table 5 shows the results of the interference coefficients for dual spillways operation under the 12 scenarios listed in Table 3. From Table 5, the values of C_I show much larger variation at low head than at high head. Also, the plot implies that the lower water levels cause a larger reduction in the outflow rate due to the interference effects from dual spillways operations.

For the numerical simulation data, a multiple regression analysis was carried out as a function of the following parameters: W, D, H_e, H_d, where H_e is the effective head upstream. As shown in Eq. (2), the distance-width ratio factor (D/W) proved to be an

Table 3. Twelve scenarios with respect to the distance-width ratio (D/W)

Model number	Distance (m)	Width (m)	D/W (m/m)
Andong-3	5	123.2	0.04
Juam-2	8	92.3	0.08
Soyang-1	10	121.0	0.09
Andong-1	34	123.2	0.28
Imha-3	78	118.8	0.66
Andong-2	104	114.8	0.91
Imha-2	162	118.8	1.36
Soyang-2	184	121.0	1.52
Soyang-3	392	121.0	3.24
Juam-1	512	92.3	5.55
Juam-3	706	92.3	6.84
Imha-1	812	118.8	7.65

Table 4. Stage-discharge rating curves for Andong-1

Spillway	Phy. H (El.m)	Phy. Q (m^3/s)	Num. H (El.m)	Num. Q (m^3/s)	Phy. H_e/H_d	Phy. Q/Q_d	Num. H_e/H_d	Num. Q/Q_d
E. spillway	154.5	610	154.1	329	0.23	0.12	0.20	0.06
	156.0	1,008	156.7	1,341	0.35	0.20	0.40	0.26
	157.2	1,502	159.4	2,513	0.44	0.30	0.60	0.50
	159.4	2,502	162.0	3,651	0.60	0.49	0.80	0.72
	160.2	3,004	164.7	5,066	0.66	0.59	1.00	1.00
	162.5	4,010	169.1	7,268	0.83	0.79	1.33	1.43
	164.3	4,770	—	—	0.97	0.94	—	—
	165.3	5,302	—	—	1.05	1.05	—	—
	165.8	5,575	—	—	1.08	1.10	—	—
	166.0	5,788	—	—	1.10	1.14	—	—
A. spillway	154.5	610	154.1	351	0.23	0.12	0.20	0.07
	155.5	1,002	156.7	1,815	0.31	0.20	0.40	0.36
	156.5	1,503	159.4	3,527	0.38	0.30	0.60	0.70
	158.2	2,504	162.0	5,217	0.51	0.49	0.80	1.03
	159.0	3,002	164.7	7,329	0.57	0.59	1.00	1.45
	160.3	4,008	169.1	10,668	0.67	0.79	1.33	2.11
	162.2	5,302	—	—	0.81	1.05	—	—
	162.9	6,011	—	—	0.86	1.19	—	—
	164.2	7,014	—	—	0.96	1.38	—	—
	165.9	8,202	—	—	1.09	1.62	—	—
D. spillway	153.6	233	154.1	646	0.17	0.05	0.20	0.13
	154.4	947	156.7	2,979	0.23	0.18	0.40	0.59
	155.1	1,587	159.4	5,680	0.28	0.30	0.60	1.12
	156.4	2,812	162.0	8,310	0.38	0.54	0.80	1.64
	156.9	3,297	164.7	11,577	0.41	0.63	1.00	2.29
	157.9	4,287	169.1	16,670	0.49	0.82	1.33	3.29
	159.3	5,721	—	—	0.59	1.09	—	—
	159.7	6,142	—	—	0.62	1.17	—	—
	160.7	7,212	—	—	0.70	1.38	—	—
	161.5	8,089	—	—	0.76	1.55	—	—
	162.5	9,212	—	—	0.83	1.76	—	—
	164.3	11,304	—	—	0.97	2.16	—	—
	164.8	11,902	—	—	1.01	2.28	—	—
	165.8	13,119	—	—	1.08	2.52	—	—

Note: Phy. and Num. = physical model and numerical model, respectively; H and Q = water surface elevation and outflow discharge, respectively; EL.m = elevation of 00.0 m; and E. spillway, A. spillway, and D. spillway = existing spillway, additional spillway, and dual spillway, respectively.

Table 5. Interference coefficients for dual spillway simulations for 12 scenarios

Model number	D/W ratio (m/m)	C_I values for H_e/H_d ratio: 0.2	0.4	0.6	0.8	1.0	1.33
Andong-3	0.04	0.932	0.940	0.933	0.926	0.920	0.912
Juam-2	0.08	0.940	0.946	0.940	0.934	0.928	0.921
Soyang-1	0.09	0.905	0.942	0.940	0.932	0.924	0.913
Andong-1	0.28	0.949	0.944	0.940	0.937	0.934	0.929
Imha-3	0.66	0.964	0.954	0.946	0.940	0.935	0.928
Andong-2	0.91	0.974	0.964	0.954	0.947	0.941	0.935
Imha-2	1.36	0.937	0.957	0.956	0.952	0.947	0.941
Soyang-2	1.52	0.956	0.963	0.959	0.954	0.950	0.943
Soyang-3	3.24	0.962	0.971	0.967	0.961	0.955	0.948
Juam-1	5.55	0.983	0.971	0.966	0.963	0.961	0.958
Juam-3	6.84	0.955	0.977	0.974	0.968	0.962	0.954
Imha-1	7.65	0.932	0.971	0.973	0.971	0.968	0.965

important model parameter at six different reservoir elevations ranging from $H_e/H_d = 0.2$ to 1.33 above the crest as shown in Figs. 8 and 9. The resulting relationship from the multiple regression analysis is

$$C_I = 1 - F_I = 0.0076\ \ln\left[\left(\frac{DH_d}{WH_e}\right)\right] + 0.9462 \qquad (2)$$

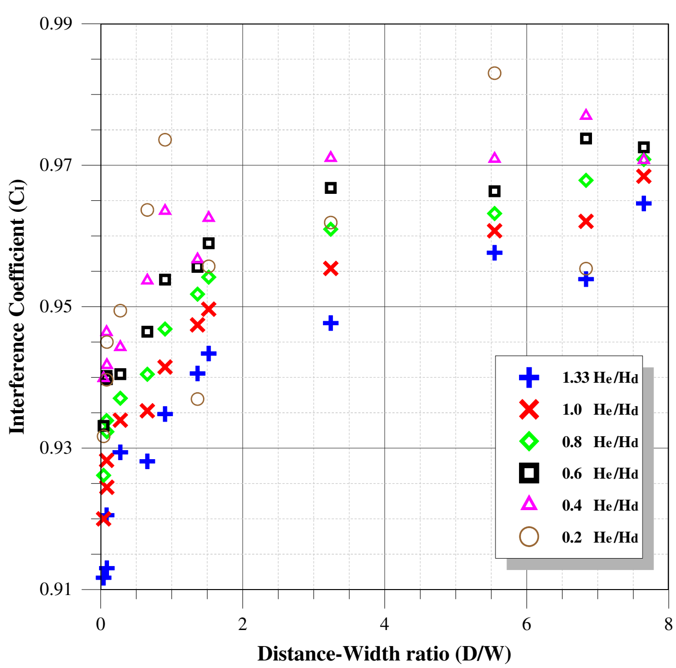

Fig. 8. Interference coefficients for dual spillways simulations with various scenarios.

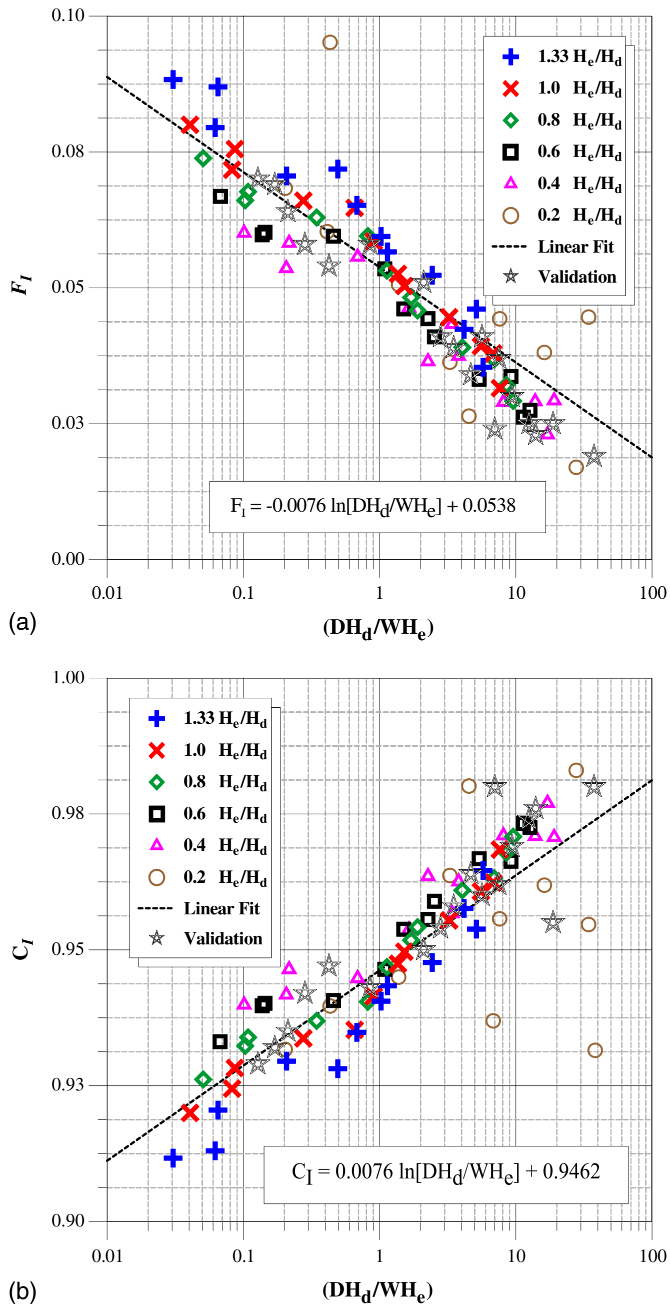

Fig. 9. Regression model for the distance-width ratio (D/W) and head ratio (H_d/H_e) by dual spillway simulations.

where C_I is the interference coefficient and for the distance-width ratio factor (D/W) and depth ratio (H_d/H_e); and F_I = discharge reduction factor. The root-mean square error is 0.0098 and the adjusted R^2 value is 0.68 at a 0.05 significance level.

Model Validation

In order to validate the interference effects of dual spillways operation, a comparative analysis using the physical and numerical model studies was carried out for a validation model equipped with a system of spillways as shown in Fig. 10. The interference coefficient of dual spillway is defined the ratio of total simultaneous outflow discharge to the summation of outflow discharges of two spillways. Following the previously performed method, the stage-discharge rating curves were computed using numerical simulation results validated by physical model study. The physical model of ogee-crest spillways of the validation model is constructed and fabricated of plexiglas walls and still bottoms considering distinctive shape of the proposed weir crest. The scale of the model is 1:70 as a follow-up to guidelines suggested by the USBR (1980) and included a tangent sectional control structures without discharge channels. Plexiglas was chosen because it could replicate smooth curves, and be clearly observed in the test facilities. Conversely, the domain for numerical modeling is 350 m wide and 350 m long, and six ogee-crest spillways are installed on the dam crest with the different size gates constructed in each spillway as shown in Fig. 10. For simulating the hydraulic performance, boundary conditions are established for the six sides of the computational space. Hydrostatic pressure was adopted for the upstream boundary condition, continuative for downstream, top symmetry, blocked obstacle (no slip) for bottom upstream, and no slip surface for ogee-crest obstacle boundary. Accordingly, five operation scenarios with respect to the topographical layouts of each spillway are set up as shown in Table 6. As a result, the resultant values of interference coefficient, which were calculated in the previous section, are applied to several patterns of spillways configuration of the validation model based on the proposed regression models. Consequently, from the overall findings by the physical and numerical model studies performed considering interference effects of dual spillway based on the proposed regression models, the results showed the similar patterns to the previous 12 results as shown in Fig. 11, and the analysis is considered to be validated. As shown in Fig. 11, the results of the interference coefficients for the validation model are also generally in good agreement with that of the regression equation.

Implication for Flood Routing in Large Reservoirs

In order to determine the impact of the interference effects of dual spillway operation on water level in a large reservoir, the computed interference coefficients were applied to a larger flood routing through the Andong multipurpose dam in South Korea. The dam is equipped with both existing and additional spillways for reservoir flood routing. For the simulation, the rainfall data provided by Korea Meteorological Administration (KMA) defined an areal average rainfall amount with a 200-year period of return. Probable maximum precipitation (PMP) was estimated by the hydrometeorological method, which consists of moisture maximization, storm transposition, and envelopment procedure, considering scientific advantage of reflecting characteristics of the basin. Following the hydrometeorological approach described previously, the final estimation of PMP of the proposed dam basin was calculated as 580 mm. Using the temporal distribution technique by Huff (1967), the given rainfall of the dam basin was allocated into the hourly values on a third-quartile peak pattern. Effective rainfall was estimated through the Natural Resources Conservation Service (NRCS) reflecting the condition of antecedent moisture condition-III (AMC-III) in order to consider extreme storm event of PMF. The rainfall-runoff simulation was conducted using HEC-HMS (3.1.3) model developed by USACE (2008). Accordingly, the PMF peak discharge of the dam basin was calculated as 15,094 m^3/s. Applying the interference coefficients of dual spillway operation to the system of spillways on the proposed dam, reservoir flood routing analysis was performed on the technical ROM condition. During the design flood the constant release-based technical ROM was selected, taking into account the flood control capacity of river downstream, while during the PMF full

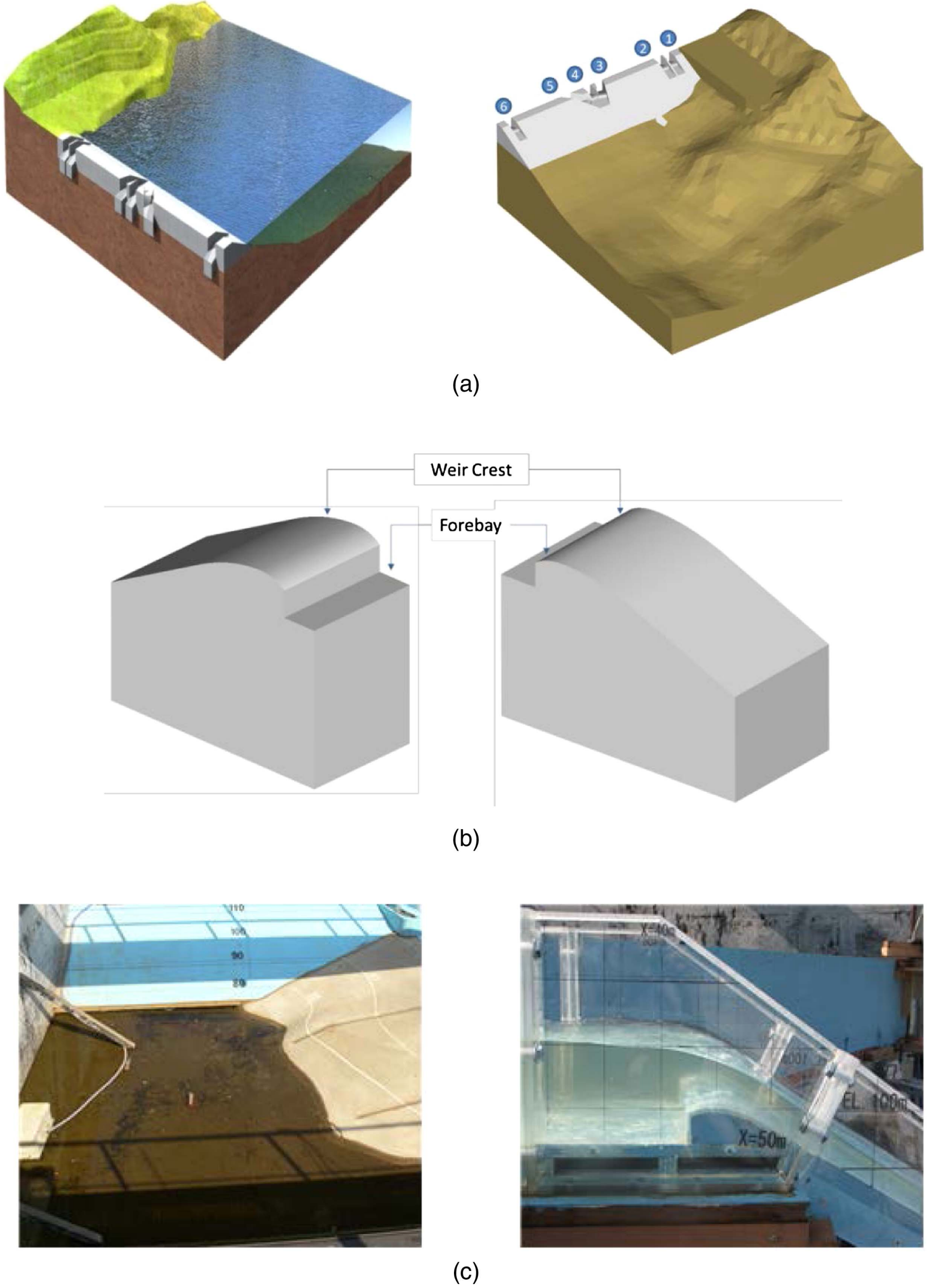

Fig. 10. Physical and numerical model validation: (a) numerical modeling; (b) solids of overflow weir of the spillway; and (c) physical models of reservoir and spillway.

opening of all spillways' gates is applied for the purpose of dam safety. The HEC-5 simulation was performed as a reservoir routing model and the results are shown in Fig. 12.

As a general result, the interference effects of dual spillway operation for a system of an existing dam are outlined as follows. For dual spillways operation, as shown in the Table 7 and Fig. 12, the reservoir water level rises to an elevation of 164.32 m without consideration of the interference coefficients. After considering the interference coefficient, the maximum water level would be 42 cm (3.3%) lower than without consideration of interference coefficients. This result indicates that it is necessary to enlarge the net width of the spillway for the dam safety. In other words, a gate with larger width on the weir crest is needed for optimal spillway design. The overall results show that the closer both existing spillway and additional spillway are located to each other, the larger is the degree of interference effects of dual spillways. Finally, we should consider the interference effects in designing the additional spillway for a dam.

Summary and Conclusions

In this study, the interference effects of dual spillways under simultaneous gate opening condition based on topographical layouts were investigated using a comparative analysis of physical model experiments and numerical model simulations. The interference coefficients for four dams and 12 configurations were analyzed. The interference coefficients were tested for Andong dam in South

Table 6. Interference coefficients for dual spillway simulations for the validation model

Model number	D/W ratio (m/m)	C_I values for H_e/H_d ratio					
		0.2	0.4	0.6	0.8	1.0	1.33
1 + 2	0.25	0.945	0.946	0.944	0.937	0.932	0.931
1 + 4	2.80	0.977	0.976	0.966	0.961	0.959	0.949
1 + 6	7.50	0.981	0.975	0.975	0.970	0.963	0.959
3 + 4	0.17	0.942	0.946	0.942	0.936	0.931	0.930
4 + 5	0.14	0.941	0.945	0.942	0.937	0.931	0.928

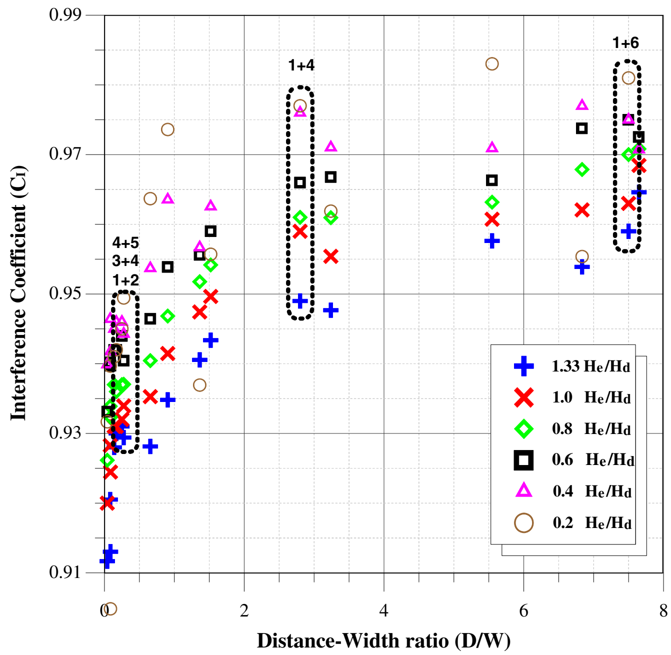

Fig. 11. Interference coefficients for dual spillways operations with various scenarios. The dashed lines indicate the results of the validation model with dual conditions of 1 + 2, 1 + 4, 1 + 6, 3 + 4, and 4 + 5.

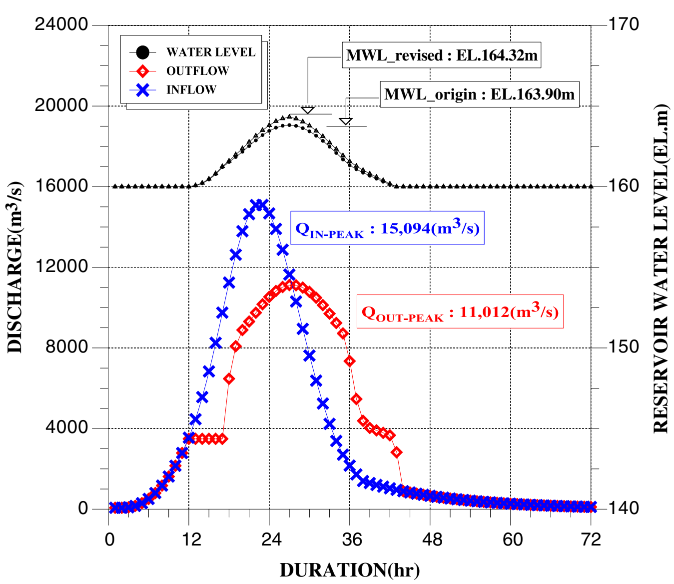

Fig. 12. Results of reservoir operations under the PMF at Andong dam.

Table 7. Results of PMF flood routing in Andong reservoir with dual operation

Classification	With C_I consideration	Without C_I consideration	Remarks
Inflow peak discharge (m^3/s)	15,094	15,094	—
Outflow peak discharge (m^3/s)	11,155	11,012	143.0 (decrease)
Maximum water level (EL.m)	163.90	164.32	42 cm (increase)

Note: EL.m = elevation of 00.0 m.

Korea using reservoir flood routing of the PMF to identify the impact of the interference effects of dual spillways operation on reservoir stage during extreme storms.

The overall results of the analysis are as follows:

- The hydraulic model study using physical model experiment and numerical model simulation for the existing and additional spillways demonstrate the effect of interference for dual spillway operations. However, when both spillways are operated at the same time the total flow rate through the two spillways can be reduced by up to 7.6% when the two spillways are close together. This implies that flow rate over the two spillways has a tendency to decrease under such conditions due to spillway interference;
- Spillway interference coefficients depend on the distance-width ratio D/W between the two spillways and the operational stage H_d/H_e. The spillway interference coefficients can be estimated from the parameter DH_d/WH_e. The comparison between calculated and measured data shows very good agreements between the physical experiments and the numerical simulations; and
- The importance of the interference coefficients was demonstrated in the simulation of the PMF at Andong dam. The reservoir flood routing showed that the water level would rise by 42 cm with the application of the discharge reduction coefficient. This indicates that it is necessary to increase the spillway width by $(1/C_I)$ for dam safety.

Notation

The following symbols are used in this paper:

A_i = area of cell face in i-direction;
$C_{E,A}$ = variable discharge coefficient of existing spillway and additional spillway;
C_I = interference coefficient;
D = separation distance between two spillways;
F_I = discharge reduction factor;
f_i = Reynolds stresses;
g_i = gravitational force;
H_d = design head;
H_e = effective head upstream above the crest including approach velocity head;
$K_{aE,aA}$ = coefficient of abutment contraction of existing spillway and additional spillway;
$K_{pE,pA}$ = coefficient of pier contraction of existing spillway and additional spillway;
$L_{E,A}$ = effective length of crest of existing spillway and additional spillway;
$L'_{E,A}$ = net length of crest of existing spillway and additional spillway;

L'_{E+A} = total net length of dual spillway crest;
$N_{E,A}$ = number of piers of existing spillway and additional spillway;
P = pressure;
Q = discharge rate;
Q_d = discharge rate at design head;
$Q_{E,A}$ = discharge of existing spillway and additional spillway;
Q_{E+A} = simultaneous outflow discharge through existing and additional spillways;
u_i = velocities in x-, y-, and z-directions;
V_F = volume of fluid in cell;
W = spillway width;
x_i = spatial coordinates; and
ρ = density.

References

Cassidy, J. J. 1965. "Irrotational flow over spillways of finite height." *J. Eng. Mech. Div.* 91 (6): 155–173.

Chanel, P., and J. Doering. 2008. "Assessment of spillway modeling using computational fluid dynamics." *Can. J. Civ. Eng.* 35 (12): 1481–1485. https://doi.org/10.1139/L08-094.

Chow, V. T. 1959. *Open-channel hydraulics*, 365–380. New York: McGraw-Hill.

Ho, D., B. Cooper, K. Riddette, and S. Donohoo. 2006. "Application of numerical modelling to spillways in Australia." In *Proc., Int. Symp. on Dams in the Societies of the 21st Century, 22nd Int. Congress on Large Dams (ICOLD)*, edited by L. Berga, et al. London: Taylor & Francis.

Huff, F. A. 1967. "Time distribution of rainfall in heavy storms." *Water Resour. Res.* 3 (4): 1007–1019. https://doi.org/10.1029/WR003i004p01007.

Kim, D. G., and J. H. Park. 2005. "Analysis of flow structure over ogee-spillway in consideration of scale and roughness effects by using CFD model." *KSCE J. Civ. Eng.* 9 (2): 161–169. https://doi.org/10.1007/BF02829067.

Koutsunis, N. A. 2015. "Impact of climatic changes on downstream hydraulic geometry and its influence on flood hydrograph routing—Applied to the bluestone dam watershed." M.S. degree, Dept. of Civil and Environmental Engineering, Colorado State Univ.

Lee, J. H., and P. Y. Julien. 2016a. "ENSO impacts on temperature over South Korea." *Int. J. Climatol.* 36 (11): 3651. https://doi.org/10.1002/joc.4581.

Lee, J. H., and P. Y. Julien. 2016b. "Teleconnections of the ENSO and South Korean precipitation patterns." *J. Hydrol.* 534: 237–250. https://doi.org/10.1016/j.jhydrol.2016.01.011.

Lee, J. H., and P. Y. Julien. 2017. "Influence of the El Niño/southern oscillation on South Korean streamflow variability." *Hydrol. Processes* 31 (12): 2162–2178. https://doi.org/10.1002/hyp.11168.

Li, S., S. Cain, N. Wosnik, C. Miller, H. Kocahan, and R. Wyckoff. 2011. "Numerical modeling of probable maximum flood flowing through a system of spillways." *J. Hydraul. Eng.* 137 (1): 66–74. https://doi.org/10.1061/(ASCE)HY.1943-7900.0000279.

MOCT (Ministry of Construction and Transportation). 2003. *Hydraulic model study of Soyanggang multipurpose dam auxiliary spillway.* [In Korean.] Governing City, South Korea: MOCT.

Olsen, N. R., and H. M. Kjellesvig. 1998. "Three-dimensional numerical flow modeling for estimation of spillway capacity." *J. Hydraul. Res.* 36 (5): 775–784. https://doi.org/10.1080/00221689809498602.

Savage, B. M., and M. C. Johnson. 2001. "Flow over ogee spillway: Physical and numerical model case study." *J. Hydraul. Eng.* 127 (8): 640–649. https://doi.org/10.1061/(ASCE)0733-9429(2001)127:8(640).

USACE (US Army Corps of Engineers). 2008. *Hydrologic modeling system HEC-HMS, user's manual version 3.2*. Davis, CA: USACE.

USBR (US Bureau of Reclamation). 1980. *Hydraulic laboratory techniques: A water resources technical publication*. Denver: US Dept. of the Interior, Bureau of Reclamation.

Yakhot, V., and S. A. Orszag. 1986. "Renormalization group analysis of turbulence. I: Basic theory." *J. Sci. Comput.* 1 (1): 3–51. https://doi.org/10.1007/BF01061452.

Yakhot, V., and L. M. Smith. 1992. "The renormalization group, the e-expansion and derivation of turbulence models." *J. Sci. Comput.* 7 (1): 35–61. https://doi.org/10.1007/BF01060210.

Zeng, J., L. Zhang, M. Ansar, E. Damisse, and J. A. Gonzalez-Castro. 2017. "Applications of computational fluid dynamics to flow ratings at prototype spillways and weirs. I: Data generation and validation." *J. Irrig. Drain. Eng.* 143 (1): 04016072. https://doi.org/10.1061/(ASCE)IR.1943-4774.0001112.

J. Hydraul. Eng., 2019, 145(5): 04019014